Chapter 15
Lithium in Medicine: Mechanisms of Action

Duarte Mota de Freitas, Brian D. Leverson, and Jesse L. Goossens

Contents

D. Mota de Freitas (✉) • B.D. Leverson • J.L. Goossens
Department of Chemistry and Biochemistry, Loyola University Chicago,
1068 West Sheridan Road, Chicago, IL 60660, USA
e-mail: dfreita@luc.edu; bleverson@luc.edu; jgoossens@luc.edu

A. Sigel, H. Sigel, and R.K.O. Sigel (eds.), *The Alkali Metal Ions: Their Role for Life*,
Metal Ions in Life Sciences 16, DOI 10.1007/978-3-319-21756-7_15

Abstract In this chapter, we review the mechanism of action of lithium salts from a chemical perspective. A description on how lithium salts are used to treat mental illnesses, in particular bipolar disorder, and other disease states is provided. Emphasis is not placed on the genetics and the psychopharmacology of the ailments for which lithium salts have proven to be beneficial. Rather we highlight the application of chemical methodologies for the characterization of the cellular targets of lithium salts and their distribution in tissues.

Keywords Bipolar disorder • Glycogen synthase kinase-3β • Lithium • Mechanisms of action

Please cite as: *Met. Ions Life Sci.* 16 (2016) 557–584

1 Introduction

Lithium (*lithos* for stone in Greek) was discovered in Sweden in the early part of the nineteenth century. It is an alkali metal and the third element on the Periodic Table. The electronic configuration of the lithium atom is $1s^2 2s^1$. The outer electron is easily removed thereby forming the lithium ion (Li^+), which has the stable electronic configuration, $1s^2$, of the noble gas helium. Its high reactivity explains why Li never exists by itself, thus accounting for its preferred occurrence as Li^+ in seawater and in minerals. In organolithium compounds, lithium forms a polar covalent bond with carbon by sharing its outer electron [1]. In non-aqueous media, organolithium compounds are a source of carbanions that are useful for the formation of carbon–carbon bonds [1]. Li and Li^+ have found important industrial applications, including the manufacture of lithium-ion batteries [2], ceramics and alloys [3], and as a source of tritium for nuclear usage [4]. The solvent in living systems is water. For lithium salts used in therapy, primarily lithium carbonate, the outer electron of Li is completely transferred to the anion to form the Li^+ cation. Henceforth, any referral to lithium signifies Li^+ and not Li, because it is Li^+ that is therapeutically relevant, and not the anion with which it forms a counterion.

Unlike other alkali and alkaline earth metal ions, such as Na^+, K^+, Mg^{2+}, and Ca^{2+}, Li^+ is only present in trace amounts in normal individuals. It therefore begs the question: How can Li^+ impact the levels of these four important ions in human physiology? General trends in ionic radii stem from their positions on the Periodic Table: (i) increases down a group due to population of additional electron shells; and (ii) decreases across a period because of a build-up in nuclear charge within an electron shell. It follows from these trends that ionic radii derived from elements that are positioned diagonally on the periodical table have similar ionic radii, the so-called *diagonal relationship*.

Table 1 Ionic radii of Li^+ and other biochemically-related radii.[a,b]

Ion	r (CN = 4)	r (CN = 6)
Li^+	59	76
Mg^{2+}	57	72
Na^+	99	102
Ca^{2+}	not available	100

[a]r, ionic radius; CN, coordination number.
[b]Data collected from [5].

In Table 1, the listed coordination numbers and the r values (in pm), are from Shannon [5]. As it is apparent from Table 1, when six ligands are bound to the central metal ion, Li^+ and Mg^{2+} have similar ionic radii; the same relationship applies to coordination number four. Both Li^+ and Mg^{2+} are hard acids that prefer hard oxygen-containing side chains of amino acids, such as aspartate, glutamate, and asparagine. It is important to note that there is a two-fold difference in the charges of the two ions. In addition to stronger binding affinities for Mg^{2+}, the differences in charge density may account for distinct preferences in coordination number and geometries (4 and tetrahedral for Li^+ [6], and, for Mg^{2+}, 6 and octahedral [7]). More details on the inorganic chemistry of Li^+ can be found in our previously published review [8].

Frausto da Silva and Williams [9] first proposed that competition between Li^+ and Mg^{2+} bound to biological molecules may be the underlying theme in Li^+ interactions in cells. This hypothesis has since been demonstrated experimentally by us and others using a myriad of spectroscopic techniques [8].

Mg^{2+} is ubiquitous in the cell and its presence is essential for the function of many enzymes and other biological processes. If Li^+ were to dislodge Mg^{2+} from its native binding sites, the cell machinery would be disrupted. It is therefore feasible that, in an Mg^{2+}-containing protein that has both high-affinity and low-affinity sites, Li^+ would compete for the low-affinity Mg^{2+} binding site. Studies using density functional theory indicate that solvent accessibility, net charge, and ligand environment of the Mg^{2+} sites may all play a part in metal ion competition [10].

For adult patients, lithium carbonate doses of 900 to 1,200 mg/day result in steady-state lithium levels in the range of 0.5 mM to 1.2 mM, which are optimal for effective maintenance of bipolar patients [11]. For tissues in a 70 kg-adult, the total and free concentrations of Mg^{2+} are, respectively, in the range of 20 mM and 0.2 mM [12]. Depending on the geographical location, the highest reported Li^+ concentration in tap water is approximately 160 μg/L, which is three orders of magnitude less than that used in the treatment of bipolar disorder and depression. Although there are only trace amounts of Li^+ in drinking water, some studies have suggested that Li^+ may aid in suicide prevention both in patients with mood disorders and in normal individuals [13]. If indeed the putative correlation between suicide prevention and lithium levels in tap water is valid, a mechanism other than ion competition at low ratios of Li^+/bound Mg^{2+} must be present.

2 Uses of Lithium in Medicine

Originally used to treat bipolar disorder, the use of Li^+ has expanded to other illnesses such as Alzheimer's disease and thyroid cancer. Although lacking specificity, Li^+ used in tandem with other medications has proven to be effective.

2.1 Bipolar Disorders

Bipolar disorders (BD) are debilitating psychiatric mood disorders characterized by repeating cycles of depression and mania. Diagnosis of each type of BD is based on meeting a strict set of criteria describing: mania, hypomania, and major depression [14]. BD type I manifests itself as a manic state, which may be followed by hypomania or major depression. This differs from BD type II, which is characterized by both a hypomanic and major depressive state, while unipolar patients suffer solely from major depression. Approximately 2 % of the world population struggles with this disease while 10–12 % commit suicide to escape the crippling emotional roller coaster [15].

It has been well established that Li^+ is effective in treating manic states. Although there have been many drugs developed to treat BD, such as valproate and lurasidone, their effectiveness varies depending on several factors, including the type of BD and unique neurological profile of the patient. With regards to BD type I disorder, after an initial delay of 1–2 weeks, Li^+ has a response rate of 70–80 % and improvement continues until it reaches a plateau at 3–4 weeks [16]. These mood stabilizing effects can continue indefinitely without recurrences and is not immediately reversible after treatment is discontinued [17]. For treatment of BD type II disorder, Li^+ efficacy is seen at 6–8 weeks [18] and its effectiveness is the greatest soon after diagnosis [19]. Although anti-psychotic drugs, such as quetiapine and olanzapine, are very effective, Li^+ is still prescribed for treatment of BD type II disorder [20].

2.2 Alzheimer's Disease

Alzheimer's disease (AD) is a common chronic form of dementia characterized by loss of memory, change in behavior, and inability to concentrate. The exact cause of AD is still unknown but identifiable histopathological trademarks have been found, such as hyperphosphorylated neuronal microtubule-associated protein (tau), amyloid plaques, and a decrease in brain-delivered neurotropic factor (BDNF). Li^+ has the unique ability to repress each of these AD phenotypes. In a cross sectional study, older BD patients undergoing chronic Li^+ treatment had a significantly lower incidence of AD compared to those untreated or the general population (3 % *versus* 19 % respectively) [21]. These findings suggest that chronic Li^+ treatment of BD patients can protect against the development of dementia-type disorders, in particular AD [22].

The precise mechanism by which Li^+ delays the progression of AD has yet to be determined. An understanding of the involvement of tau in AD is emerging. Tau protein promotes and stabilizes microtubule formation, a process that is regulated by glycogen synthase kinase 3 (GSK-3). In AD patients, tau has been found to be hyperphosphorylated by GSK-3, causing the formation of paired helical fibers and the weakening of the cytoskeleton [23]. Li^+ reduces GSK-3-induced tau phosphorylation at multiple epitopes in both transfected cells and in neurons [24, 25]. The effects are both time- and concentration-dependent and effective at 1 mM and 3 mM. It was also demonstrated that Li^+-induced changes in tau phosphorylation are not the result of neurotoxicity, since even at 25 mM Li^+ hippocampal cell morphology was unaffected and the changes in tau phosphorylation were entirely reversible [24, 25].

Like tau proteins, amyloid β-peptides (Aβ) are thought to be one of the primary factors that contribute to AD. In recent years, the connection between Aβ plaques and AD has been called into question because the concentration of Aβ is not correlated to the degree of cognitive impairment observed in AD subjects. Preceding the onset of pathology, Li^+ decreased the rate of formation of toxic plaques, and prevented degeneration of memory in a PS1xAPP mouse model [26]. Another group found that inhibition of GSK-3 with Li^+ led to a decrease of the concentration of amyloid precursor protein by enhancing its degradation [27]. Although in both of these studies Li^+ appeared to act as an inhibitor, there were other investigations that contradicted these results [28, 29].

Due to the neuroprotective effects observed in BD patients, it has been proposed that Li^+ could be used to treat AD. Clinical trials have begun to investigate the effect Li^+ has on AD patients. Li^+ has been shown to increase BDNF, which has been linked to a delay and/or stagnation of the cognitive impairment symptoms in AD patients [30, 31].

2.3 Thyroid Cancer Treatment

Effects of Li^+ on patients with thyroid cancer are well documented and give insight on possible mechanistic pathways. Patients undergoing Li^+ treatment have a higher probability of developing hyperthyroidism. This side effect can be useful because Li^+ can inhibit thyroid hormones and increase retention of radioactive iodine. Therefore, Li^+ can be used as an adjunctive therapy in the treatment of hyperthyroidism and thyroid cancer [32, 33].

Li^+ is thought to inhibit coupling of iodotyrosine residues in the formation of thyroxine (T4) and triiodothyrosine (T3), which control the release of iodothyronines. Li^+ may also affect deiodinase activity, which originates from a group of enzymes that activates thyroid hormones by converting T4 to T3, or inactivate hormones by converting either T4 to reverse triiodothyronine or T3 into inactive diiodothyronine [32]. In addition, Li^+ can participate in a feedback loop mechanism by increasing intrathyroidal iodine, and inhibiting the release of T3 and T4.

The excretion of thyroid hormones leads to a decrease of T3 and T4 levels in serum during iodine therapy [33, 34]. Due to this feedback loop, iodine retention is increased without interfering with iodine uptake, increasing radioactive iodine concentration in normal and cancer thyroid cells [35].

3 Methods of Lithium Detection

3.1 Overview of Tools for Lithium Detection

Analytical methods available for the direct detection of Li^+ in blood and other tissues fall under two categories: (i) those that measure *total* Li^+ concentrations (atomic absorption or flame emission spectrometry, inductively-coupled plasma mass spectrometry, solution ^{7}Li NMR (nuclear magnetic resonance spectroscopy) and solution ^{7}Li MRSI (magnetic resonance with spectroscopic imaging)) and (ii) those that detect *free* Li^+ concentrations (optical or fluorescence indicators, ion-selective microelectrodes, solution ^{7}Li NMR and solid-state ^{7}Li NMR). If competition between Li^+ and bound Mg^{2+} were present, an increase in total Li^+ concentration, $[Li^+]_{total}$, would increase the concentration of free Mg^{2+}, $[Mg^{2+}]_{free}$, and decrease the concentration of bound Mg^{2+}, $[Mg^{2+}]_{bound}$, with the total Mg^{2+} concentration, $[Mg^{2+}]_{total}$, remaining intact.

The total concentrations of Li^+ in blood of bipolar patients on lithium therapy are well within the detection limits of atomic absorption or flame spectrometry, making them the methods of choice for assessing drug response and toxicity in the clinic, as well as patient compliance. The principles of atomic absorption and flame spectrometry are beyond the scope of this chapter, and for more details the reader is referred to an earlier review on these methodologies [36].

Li^+-selective chromophores, fluorophores, and microelectrodes have been designed based on the premise that, relative to other alkali and alkaline earth metal ions, some crown ethers and cryptands selectively bind Li^+ [37]. However, the large excess of Na^+ over Li^+ in biological fluids and the low Li^+/Na^+ selectivity ratio place limitations on the usefulness of these methods for measuring free Li^+ concentrations, $[Li^+]_{free}$.

The principles behind other more informative methods, such as ^{7}Li NMR spectroscopy and ^{7}Li MRSI, or indirect detection of Mg^{2+} with the aid of fluorophores, are explained below, and their applications are described thereafter in this chapter. Before continuing with the description of these spectroscopic methods, it is important to point out that no radioactive isotope of lithium exists. Also, Li^+ and Mg^{2+} have no unpaired d electrons, and therefore they are not amenable to study by UV-Vis spectroscopy and electron paramagnetic resonance. In addition, Li^+ only has two valence electrons and thus, Li^+ bound to proteins cannot be detected directly by X-ray crystallography. Indeed, no crystal structure with bound Li^+ has been deposited in the Protein Data Bank. In contrast, the higher electron density of Mg^{2+} enables the investigation by X-ray diffraction of Mg^{2+} binding sites in proteins, as shown in the crystallographic structures described in Section 5.

3.2 Lithium Nuclear Magnetic Resonance Spectroscopy

In a one-dimensional NMR experiment, a sample is placed in a magnetic field and transitions among nuclear states are induced by pulses of radiofrequency; between successive pulses, a delay is required to allow for decay of the net magnetization from excited states to the ground state, a process that is quantified by spin-lattice (T_1) and spin-spin (T_2) relaxation times [38]. NMR-active nuclei have a nuclear spin, I, greater than zero, but, when I is larger than ½, quadrupolar relaxation occurs, resulting in broad lines.

Two Li isotopes exist, ^{7}Li and ^{6}Li, with natural abundances of 92.6 % and 7.4 %; because their nuclear spin values are 3/2 and 1, respectively, either nucleus can be detected by NMR spectroscopy. The quadrupole moments of both nuclei are relatively small, resulting in relatively sharp peaks [38]. In a magnetic field of 11.7 Tesla (in which ^{1}H resonates at 500 MHz), the resonance frequency for ^{7}Li is 194.3 MHz and 73.6 MHz for ^{6}Li. These frequencies are easily attainable with multinuclear NMR probes. Receptivity, the product of the natural abundance and the inherent sensitivity of a nucleus, provides insight on the easiness for the detection of a specific nucleus; relative to ^{1}H, the receptivities of ^{7}Li and ^{6}Li are, respectively, 0.27 and 6.31×10^{-4}. The T_1 values for ^{7}Li are in the msec range whereas those for ^{6}Li can be as large as one sec.

Two useful parameters in NMR spectroscopy are the chemical shift and the spin-spin coupling constant. From the number and positions of the chemical shifts, which are reported relative to a reference compound and expressed in ppm, one can garner structural information. Multiplet patterns in one-dimensional NMR spectra or cross-peaks in two-dimensional NMR spectroscopy are indicative of interactions between spins of different nuclei.

For organolithium compounds, Li atoms in distinct chemical environments exhibit different chemical shift values [39]. Similarly, depending on the nature of the carbon substituents, Li-C covalent bonds exhibit multiplets or cross peaks that result from coupling between ^{6}Li (and less often with ^{7}Li) and ^{13}C. Because the T_1 values of ^{6}Li are longer than those of ^{7}Li, solution and solid-state ^{6}Li NMR is preferable to ^{7}Li NMR for the structural analysis of organolithium compounds [39].

As a result of the larger natural abundance of ^{7}Li relative to ^{6}Li, solution ^{7}Li NMR spectroscopy is the method of choice for probing Li^+ within the 0.5 mM to 1.2 mM range used in therapy. In the cytosol, Li exists as a tetra- or hexaaqualithium(I) ion. Once bound to biomacromolecules, such as proteins or cell membranes, it is primarily present as a partially hydrated Li^+ ion. Consequently, the Li^+ environment in biological aqueous media does not vary greatly, resulting in a narrow and, for the most part, uninformative scale of chemical shift values. For example, in a solution ^{7}Li NMR study of Li^+ binding to inositol monophosphatase (IMPase), a small downfield shift of approximately 0.1 ppm was observed at a [protein]/[Li^+] ratio of *ca.* 4 [40]. In contrast, a magic-angle spinning, solid-state ^{7}Li NMR study of Li^+ binding to lyophilized *E. coli* IMPase resolved $[Li^+]_{free}$, $[Li^+]_{bound}$, and non-specifically bound Li^+ [41]. Because of the lack of covalent bonding between Li^+ and water or

other hard oxygen-containing ligands, spin-spin coupling between the quadrupolar ^{7}Li nucleus and ligand hydrogens is not observed in solution [42].

However, useful information can be obtained from chemical shifts. Figure 1A [43] shows that, in a red blood suspension, intracellular Li^{+} cannot be distinguished from extracellular Li^{+}. Representative lanthanide shift reagents, such as dysprosium triphosphate, $[Dy(PPP)_2]^{7-}$, or thulium 1,4,7,10-tetraazacyclodecane-*N,′N″,N‴*-tetramethylenephosphonate, $[HTm(DOTP)]^{4-}$, are, as a virtue of their high negative charge, impermeable through the hydrophobic interior of a cell membrane. Therefore, these reagents only shift the extracellular pool of Li^{+}; see Figure 1B for an example of packed red blood cells (RBCs) suspended in an isotonic medium containing $[Dy(PPP)_2]^{7-}$. A control experiment using coaxial tubes confirm the assignments (Figure 1C).

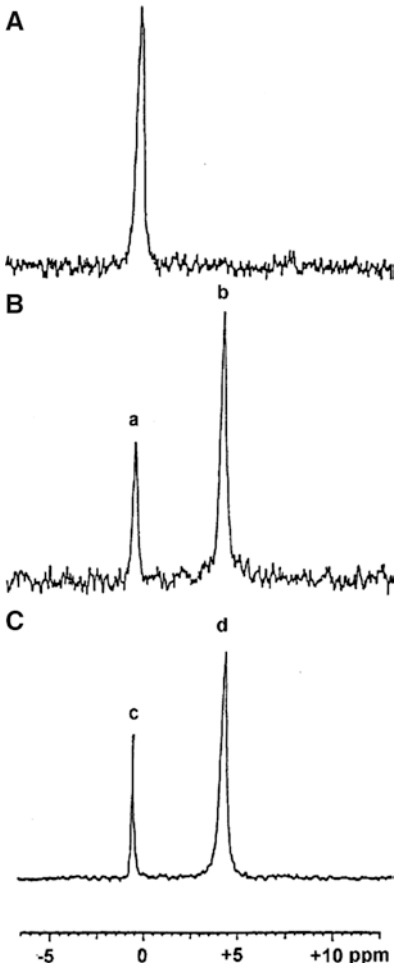

Figure 1 (**A**) ^{7}Li NMR spectrum (104.8 MHz, 37 °C) of gently packed RBCs (hematocrit was 13 %) in a medium containing 140 mM Na^{+}, 5 mM K^{+}, 3.5 mM Li^{+}, 10 mM glucose, and 50 mM HEPES at pH 7.5. Packed RBCs were incubated with 3.5 mM Li^{+} at 37 °C for 12 h prior to NMR measurements. (**B**) ^{7}Li NMR spectrum of the same RBC suspension as in part A with the exception that 5 mM $Na_7Dy(PPP)_2$ was present in the medium instead of 50 mM NaC1. (**C**) ^{7}Li NMR spectrum of a concentric sample (5-mm inner tube inside a 10-mm outer tube) containing 20 mM Li^{+} in the inner tube while the outer tube contained the same suspension medium as in part B. Labels a and c represent inner pools of Li^{+} while b and d denote outer pools. Reproduced with permission from [43]; © copyright 1987, American Chemical Society.

The T_1/T_2 ratio is a measure of Li^+ immobilization. For $[Li^+]_{free}$, where the Li^+ rotational correlation time, τ_c (which is a scale of Li^+ motion) is short relative to the its NMR resonance frequency ω ($\omega\tau_c \ll 1$), $T_1 \approx T_2$. When Li^+ is immobilized in cells, τ_c is larger, and $\omega\tau_c \gg 1$, T_1 is longer than T_2 [44]. Determination of Li^+ binding constants, K_{Li}, to cellular fractions can be calculated as follows:

$$\frac{1}{\Delta R} = \frac{1}{(R_{obs} - R_{free})} = \frac{1}{K_{Li}[B](R_{bound} - R_{free})} + \frac{[Li^+]_{total}}{[B](R_{bound} - R_{free})} \quad (1)$$

where $[Li^+]_{total}$ and [B] are the concentrations of Li^+ and binding sites. R_{obs}, R_{free} and R_{bound} are, respectively, the values of the relaxation rates (the reciprocals of relaxation times), observed for the sample itself, with saturating $[Li^+]$, or with bound Li^+. From a James-Noggle plot [45], in which ΔR^{-1} is plotted against $[Li^+]_{total}$, K_{Li} can be calculated.

3.3 Lithium Magnetic Resonance with Spectroscopy Imaging

Unlike ^{7}Li NMR, ^{7}Li MR with spectroscopy imaging (MRSI) uses a fixed magnetic field and magnetic field gradients affording the opportunity to map distribution of Li^+ in organs, including human brains. T_1-weighted measurements enhance image resolution [46].

3.4 Indirect Fluorescence Detection

The levels of free Mg^{2+}, $[Mg^{2+}]_{free}$, can be measured by using Mg^{2+}-selective fluorescent dyes, such as furaptra [47]. As Figure 2 [48] indicates, indirect fluorescence detection of $[Mg^{2+}]_{free}$ can be used for probing competition between Li^+ and bound Mg^{2+} in biological samples, with $[Mg^{2+}]_{free}$ being calculated as per equation (2) [48]:

$$[Mg^{2+}]_{free} = \frac{K_d S_{min}(R - R_{min})}{S_{max}(R_{max} - R)} + [Li^+]_{free}\frac{K_d S'_{max}(R - R'_{max})}{K'_d S_{max}(R_{max} - R)} \quad (2)$$

where K_d and K'_d are, respectively, the dissociation constants of the furaptra complexes with Mg^{2+} and Li^+; S_{min}, S_{max} and S'_{max} are the fluorescence intensities at 374 nm in the absence and in the presence of saturating concentrations of Mg^{2+} and Li^+; and R, R_{min}, R_{max}, and R'_{max} are the fluorescence intensity ratios (342 nm/374 nm) observed for the sample, and in the absence and in the presence of saturating amounts of Mg^{2+} and Li^+. Competition between Li^+ and Mg^{2+} bound to a protein could be determined by adding a third term to equation (2) [49].

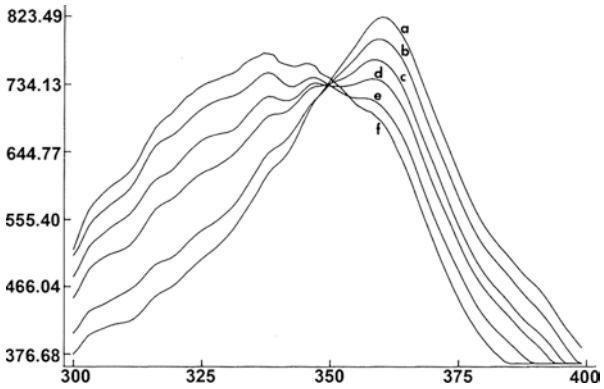

Figure 2 Fluorescence excitation spectra of 2 μM furaptra in a solution containing 5.0 mM ATP, 2.5 mM $MgCl_2$, 150 mM Tris-Cl (pH 7.4) and (a) 0 mM LiCl, (b) 5 mM LiCl, (c) 10 mM LiCl, (d) 20 mM LiCl, (e) 50 mM LiCl, and (f) 100 mM LiCl. Reproduced with permission from [48]; © copyright 1987, American Chemical Society.

4 Lithium in Living Systems

4.1 Lithium Transport Across Cell Membranes

Li^+ measures using atomic absorption and flame emission spectrophotometry may be error-prone because blood processing steps, such as centrifugation and cell lysis, may result in additional transmembrane Li^+ transport during sample preparation. ^7Li NMR studies are advantageous because cell suspensions can be investigated non-invasively. Figure 1 shows how RBC suspensions have been studied in this way. For nucleated cells (Figure 3 [50]), such as human neuroblastoma SHSY-5Y cells, continuous perfusion with aerated medium of gel-anchored cells is however required.

Li^+ uptake by RBCs takes place via a leak pathway, and through the transmembrane Cl^- exchanger or band 3 protein. The leak pathway contributes 70 % toward Li^+ influx and is thought to occur via water pores in the RBC membrane. In principle, a Li^+ cation could not use the Cl^- exchanger whose function is to transport Cl^- anions. However, CO_3^{2-} is believed to form an ion pair with Li^+, $[LiCO_3]^-$, resulting in net Li^+ influx in exchange with Cl^- efflux. Li^+ efflux from Li^+-loaded RBCs (for example, RBCs from blood of bipolar patients on Li^+ therapy), is mediated by the Na^+/Li^+ countertransporter. When the $[Na^+]$ gradient that it generated by active transport-mediated by Na^+/K^+-ATPase is partially dissipated, Li^+ efflux against a $[Li^+]$ gradient occurs, indicating that the Na^+/Li^+ countertransporter provides secondary active transport for Li^+. We later found out that Na^+/Li^+ countertransport is mediated by the Na^+/H^+ exchange protein located in the RBC membrane [51]. Mediation of Li^+ transport through other pathways, such as Na^+/K^+ cotransporter and Na^+/K^+-ATPase, has been reported; however, it does not occur at physiological concentrations of Na^+ and K^+.

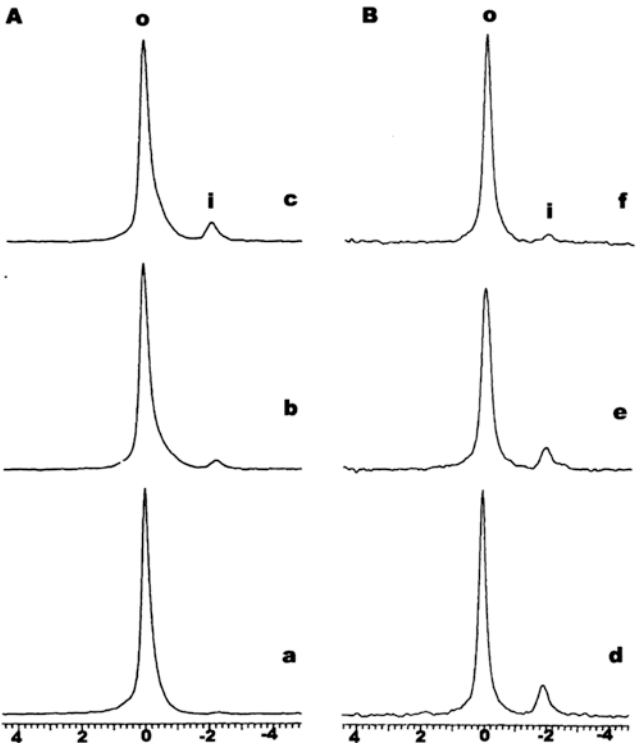

Figure 3 (**A**) ^{7}Li NMR spectra of Li^+ influx into human neuroblastoma SH-SY5Y cells embedded in agarose gel threads in a medium containing 3 mM $[HTmDOTP]^{4-}$ and 15 mM Li^+ at 11 min (spectrum a), 39 min (spectrum b) and 133 min (spectrum c) after starting the perfusion. (**B**) ^{7}Li NMR spectra of Li^+ efflux from Li^+-loaded cells at 75 min (d), 90 min (e), and 120 min (f). The symbols i and o denote the intracellular and extracellular ^{7}Li NMR signals. Reproduced with permission from [50]; © copyright 2002, John Wiley & Sons.

It was earlier speculated that the rates of Na^+/Li^+ countertransport in RBCs of bipolar patients undergoing Li^+ treatment were slower than for normal individuals, and that Li^+ ratios ($[Li^+]_{RBC}/[Li^+]_{plasma}$) were elevated for the patients. However, the rates of Na^+/Li^+ countertransport and of Li^+ ratios in RBCs of bipolar patients before and after undergoing chronic Li^+ therapy were not significantly different, indicating that the previously reported differences for RBCs of bipolar patients were not biological markers but a result of Li^+ treatment. Hypertensive patients have unequivocally shown to have significantly elevated rates of RBC Na^+/Li^+ countertransport relative to normotensive controls [52]. The cofounding effect of hypertension make earlier data from studies with RBCs of bipolar patients difficult to interpret. Details on RBC Li^+ transport pathways and their potential abnormalities have been previously described [36].

Instead of testing whether differences in rates of RBC Na^+/Li^+ countertransport and Li^+ ratios are biological markers, we studied RBCs from thirty Li^+-treated bipolar

patients and found significant correlations between Li^+ affinity to the RBC membrane, as calculated from T_1 measures, and response to and toxicity of Li^+ therapy [53].

Figure 3 illustrates how Li^+ uptake and efflux can be monitored in eukaryotic cells, in this case human neuroblastoma SHSY-5Y cells [50]. Because oxygen is required for their viability, the cells, which were anchored on gel threads, were continuously perfused with an aerated medium. Addition to the medium of veratridine, a known inhibitor of voltage-sensitive Na^+ channels, reduced the rates of Li^+ uptake and efflux, suggesting that Li^+ transport may be mediated *via* Na^+ channels. A follow-up study indicated that 40 % of Li^+ uptake in the same cell line takes place *via* the Na^+/Ca^{2+} exchanger, with the leak pathway providing the remaining balance [54].

4.2 Cellular Accumulation of Lithium

We have used T_1/T_2 ratios to investigate Li^+ immobilization in intact human RBCs and in neuroblastoma SHSY-5Y cells, as well as in their cellular components [50, 55]. The cytosol and other subcellar fractions are viscous. Therefore, the viscosity of all fractions was adjusted to 5 cP (centipoise) by addition of glycerol. Under these conditions, a 3.0 mM viscosity-adjusted LiCl solution gave a T_1/T_2 ratio of approximately of 1. Table 2 indicates that the ratio is larger in intact SHSY-5Y cells than in RBCs, presumably because there are organelles present in the former that are absent in the latter. From the T_1/T_2 ratio values in subcellular fractions from SHSY-5Y cells, we concluded that the order of Li^+ immobilization is: plasma membrane $\gg$ microsomal membrane $>$ nuclear membrane [50, 55].

We used the fluorescent dye furaptra to investigate Li^+/Mg^{2+} competition in human neuroblastoma SHSY-5Y cells. Chronic incubation of the cells for 24 to 72 hours with Li^+ resulted in a significant increase in $[Mg^{2+}]_{free}$, leading credence to the competition mechanism between Li^+ and bound Mg^{2+} in the therapeutic range (0.7 to 1.5 mM) [56].

Table 2 T_1/T_2 ratios for intact RBCs and SHSY-5Y cells as well as their subcellular fractions.[a]

Sample	$[Li^+]$ (mM)	T_1/T_2 ratio
RBCs	3.5	14
SHSY-5Y cells	2.9	100
RBC membrane	3.0	52
SHSY-5Y membrane	3.0	42
Cytosol-free homogenate	4.0	74
Cytosol-enriched fraction	4.0	6
Plasma-membrane fraction	4.0	106
Nuclear-membrane fraction	4.0	26
Mitochondrial-enriched fraction	4.0	14
Microsome-enriched fraction	4.0	52

[a]Data collected from [50] and [55].

4.3 Distribution of Lithium in Tissues

^{7}Li NMR has been used to study brains from patients with limited success; the images were however concentrated on wide brain slices or were unlocalized [57]. In contrast, with ^{7}Li MRSI, high-resolution images from brains of bipolar patients were obtained that allowed the determination of $[Li^+]_{total}$ and the observation of non-uniform Li^+ distribution [46]. Figure 4 [46] shows Li^+ brain maps from the same patient two weeks apart. In the first visit (Figure 4a), serum $[Li^+]$ was 0.3 mM lower than in the second visit for which the two sets of images were reproducible (Figures 4b and 4c). The detection of uneven Li^+ distribution in the brain of Li^+-treated bipolar patients is intriguing in that it may lead to the exploration of brain regions that are associated with emotion. This and similar studies show the promise on how Li^+ distribution can be investigated using Li^+ MRSI.

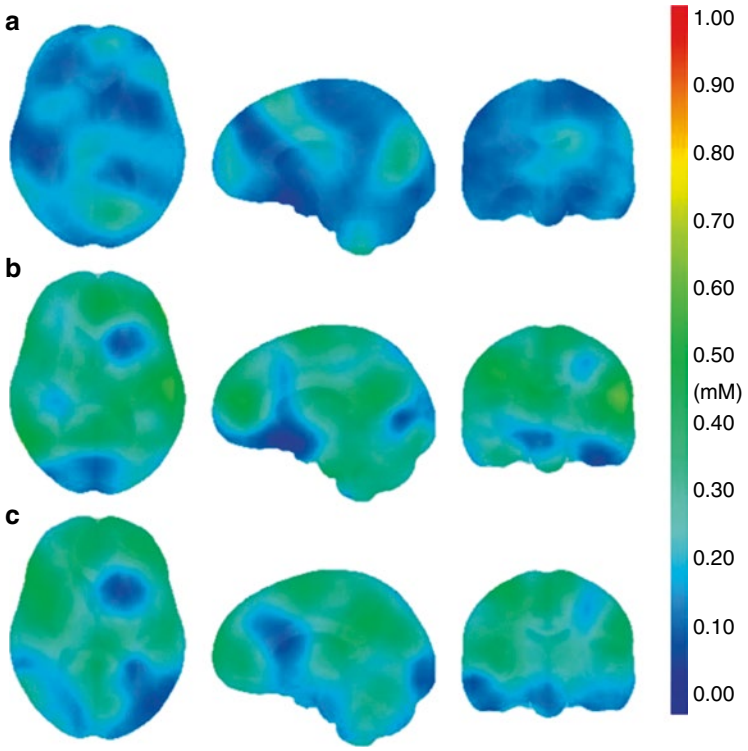

Figure 4 Comparison of Li^+ brain maps obtained from the same patient at visits two weeks apart. In the first visit (**a**), serum $[Li^+]$ was 0.5 mM, and, in the second visit, the two sets of images were at serum $[Li^+]$ of 0.8 mM (**b** and **c**). Reproduced with permission from [46]; © copyright 2012, John Wiley & Sons.

4.4 Lithium Toxicity

For most drugs, the concentration at which toxicity sets in is several orders of magnitude larger than the pharmacological level. In contrast, lithium treatment has to be monitored closely because at 2.0 mM significant side effects and toxicity occur, including, among others, weight gain, blurred vision, tremor [58], and, if left untreated, seizures and renal failure [59].

Weight gain impacts treatment compliance, and so do dermatologic side effects. Due to its high charge density, Li^+ has a very high hydration energy, which may account for the reported weight gain [60] and cutaneous adverse conditions [61].

5 Cellular Targets of Lithium

Considering the number of enzymes that utilize a magnesium cofactor, Li^+ acts on relatively few cellular targets. Curiously, Li^+ seems to mostly target enzymes associated with psychiatric disorders. This section provides an overview of the research into the mechanisms of action of Li^+ on some of the better studied Mg^{2+}-containing targets (Figure 5).

Li^+ inhibition is not limited to competition with the Mg^{2+} cofactor. Alternate mechanisms are thought to occur. This is the case for proteins such as the transcriptional factor cAMP response element-binding protein (CREB) [62, 63].

5.1 Guanine Nucleotide Binding Proteins

5.1.1 Mechanism and Li^+ Inhibition

Guanine nucleotide binding proteins (G-proteins) are regulatory membrane-bound proteins that play an indispensable role in transferring extracellular information across the cell membrane to affect intercellular functions. G-proteins are heterotrimeric in that they are composed of an α subunit (G_α), which regulates the activity of the effector protein, and a βγ subunit complex. G-proteins are attached to G-protein coupled receptors (GPCR), which are a type of hepta-helical serpentine transmembrane domain receptors. G-proteins regulate intracellular signaling cascades in response to specific GPCR activation by neurotransmitters or hormones. Once activated, GPCRs induce conformational changes in the G_α subunits, which contain the guanine nucleotide, resulting in exchange of GDP for GTP and dissociation of the βγ dimer. The dissociated α subunit then binds to its specific effector where it will stimulate or inhibit. This process is self-regulated with hydrolysis of bound GTP to GDP, effectively deactivating G_α and reforming the heterotrimeric GDP-bound G-protein conformation [64]. G_α subunits are separated into 4 primary classes based on their

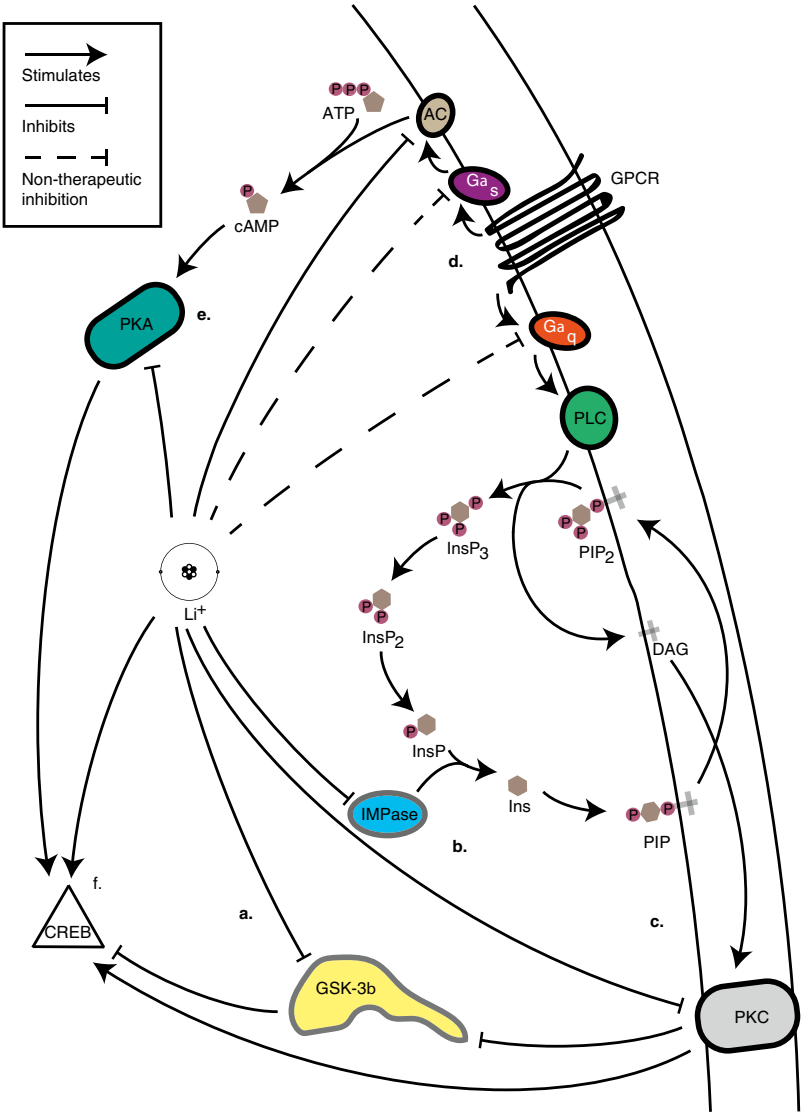

Figure 5 Li^+ affects many cellular pathways. (**a**) Li^+ is a noncompetitive inhibitor of GSK. (**b**) The PI signalling pathway is inhibited by IMPase, which prevents the cell from producing the secondary messengers DAG and PIP_2, further limiting the activity of downstream signaling proteins such as PKC. (**c**) The down regulation of MARCKS by Li^+ interrupts PKC signaling. (**d**) G-proteins $G_{\alpha s}$ and $G_{\alpha q}$ activate AC and PLC, respectively. (**e**) AC is inhibited both directly by Li^+ and indirectly by $G_{\alpha s}$. (**f**) The transcription factor CREB is activated by Li^+. AC, adenylyl cyclase, ATP, adenosine 5′-triphosphate, CREB, cAMP response element-binding protein, cAMP, cyclic AMP, DAG, 1,2-diacylglycerol, GPCR, G-protein coupled receptors, GSK-3, glycogen synthase kinase-3, IMPase, inositol monophosphatase, ($InsP_3$), 1,4,5-inositol triphosphate, ($InsP_2$), 4,5-inositol bisphosphate, (InsP), inositol phosphate, Ins, inositol, PI, phosphatidylinositol, (PIP_2), phosphatidylinositol 4,5-bisphosphate, PKA, protein kinase A, PKC, protein kinase C.

structure, G_i, G_s, G_q, and G_{11}. Each can be further separated into several different subgroups. The subunits G_s and G_i, which are involved in stimulation and inhibition of adenylyl cyclase, respectively, and G_q [64, 65], which stimulate IMPase.

In rat cortex membranes, adrenergic and cholinergic activation of G_s and $G_{i\alpha1}$, respectively, was reported to be inhibited by Li^+ [65]. In bipolar patients, G_s was postulated to be associated with mania whereas $G_{i\alpha1}$ with depression. Li^+ inhibition of G_s would result in a decrease in mania, while Li^+ inhibition of $G_{i\alpha1}$ would alleviate depression. Because G_s and $G_{i\alpha1}$ are Mg^{2+}-containing proteins, Li^+ competition for Mg^{2+} bound to these G-proteins might explain the effects of Li^+ on mania and depression.

Originally G-protein involvement in both manic and depressive cycles offered a simple and yet elegant explanation for Li^+ action in BD [66–68]. The hypothesis of Li^+ inhibition of G-proteins in BD was primarily based on cadaver and animal studies at therapeutic concentrations [65]. Studies have shown inhibition of $G_{i\alpha1}$ to be negligible and not enough to produce the significant change observed in Li^+ treatment of BD [69]. However, these reports are in conflict with others [67, 70]. Several laboratories have examined deceased patients with mood disorders that were untreated or treated with Li^+. These studies focused on G-protein concentration and function. Conflicting data indicate increased levels of $G_{\alpha s}$, $G_{i\,\alpha2}$, and $G_{\alpha1/2}$ for patients with major depression [71] and increased $G_{\alpha s}$ and $G_{\alpha q}$ for BD [72], while many other studies showed no change in any G-protein concentration [68, 73]. Intrinsic variables, such as tissue storage, patient's age, and the inability to diagnose BD or major depression via tissue samples may account for these variances [65]. Furthermore, animal studies originally showed inhibition of G-proteins, but discrepancies and inconsistencies in the reported data have led to the conclusion that the results are not reproducible [74]. Lacking a universally accepted animal model for BD, makes drawing conclusions on therapeutic effects of Li^+ tenuous and the relevancy to BD debatable [74]. Although G-proteins are no longer the main focus of Li^+ inhibition in BD, they still remain a viable player in long-term treatment efficacy [75, 76].

G-proteins are Mg^{2+}-dependent and our recent fluorescence study on G_s and $G_{i\alpha1}$ indicated that they contain two Mg^{2+} binding sites, one with high affinity and one with lower affinity. However, crystallographic reports of $G_{\alpha s}$ and $G_{i\alpha1}$ only showed the presence of one Mg^{2+} binding site [77–82]. However, these studies were conducted at very high [Li^+], which may have displaced Mg^{2+} from the low affinity Mg^{2+} site. Interestingly, for Ral, a monomeric G-protein, its crystal structure obtained in polyethylene glycol depicts two Mg^{2+} binding sites [83]. Regardless of their participation in Li^+ action in BP patients, G-proteins are therefore invaluable systems for studying Mg^{2+}/Li^+ competition due to being well characterized.

5.1.2 Li^+ Inhibition of Adenylyl Cyclase

Adenylyl cyclase (AC) is a membrane-bound enzyme responsible for converting adenosine triphosphate (ATP) to 3′,5′-cyclic adenosine monophosphate (cAMP), which serves as a secondary level of amplification of many signal transduction cycles. The increase of cAMP induces multiple effects, including opening of Ca^{2+}

channels and activation of protein kinase A (Figure 5). Li^+ is thought to inhibit AC in two ways, first by competing for its Mg^{2+} binding site or by inhibiting $G_{\alpha s}$, which is a known stimulator of cAMP formation [69]. The formation of forskolin-induced cAMP has been shown to be inhibited by Li^+ at therapeutic concentration in cerebral rat cortex [84]. In a study of euthymic BD patients undergoing Li^+ treatment, 0.5 mg of epinephrine, which is known to activate $G_{\alpha s}$ and stimulate the formation of cAMP, the plasma cAMP levels were lower when compared to untreated patients [85]. Similar studies in rodents showed a decrease in cAMP levels in cerebral cortex slices of rats treated with 2 mM of Li^+ [86] and at 1 mM Li^+ in guinea pig cortex [87, 88].

There are 10 isoforms of AC each having a different inhibition response to Li^+. Of these isoforms, AC-II, AC-V, and AC-VII are responsible for epinephrine-signal amplification and have been shown to be hypersensitive to Li^+ inhibition. Therefore, they have been implicated as being part of the array of the mechanisms of action for Li^+ treatment of BD [84, 89]. AC-V in particular is found in specific areas of the brain, including the nucleus accumbens and basal ganglia, which are associated with emotional responses. Further experiments using AC-V knock-out mice showed reduced mobility when performing the swim test, in which reduced mobility indicates BD-like behavior [84].

5.2 Inositol Monophosphatase

5.2.1 Phosphoinositide Turnover

Inositol phospholipids are the components of the phosphoinositol (PI) cycle. They represent an important class of secondary messengers, which are involved in triggering the formation and release of intracellular messengers that are vital for physiological responses within cells. Figure 5b outlines the PI cycle which is initiated by the activation of phospholipase C (PLC) by the α subunit of a specific G-protein, Gq, resulting in the conversion of phosphatidylinositol 4,5-bisphosphate (PIP_2) into 1,4,5-inositol triphosphate ($InsP_3$) and 1,2-diacylglycerol (DAG). DAG modulates the activity of protein kinase C (PKC) and $InsP_3$ induces the release of the secondary messenger Ca^{2+} [90]. The secondary messengers are then recycled and at the center is inositol monophosphatase (IMPase). IMPase catalyzes the hydrolysis of inositol derivatives and plays a crucial role in physiological response by maintaining the cellular levels of inositol (Ins), which is a precursor for many secondary messengers including DAG and PIP_2 [91].

5.2.2 Li^+ Inhibition of Inositol Monophosphatase

Mammalian IMPase is a highly conserved homodimer in which each 30 kDa subunit contains a key secondary structural feature of five alternating α-helices and β-sheets [92]. IMPase requires a trinuclear Mg^{2+} cofactor to function and is inhibited by Li^+ in

an uncompetitive manner with an inhibitor constant (K_i) of 1.0 mM [40, 93]. Inhibition is thought to involve Li^+ binding to the enzyme-substrate complex and partial displacement of the Mg^{2+} cofactor [94]. As for G-proteins (see section 5.1), IMPase crystals collected from high-salt solutions showed only one Mg^{2+} site [95]. A subsequent study in which IMPase crystallization was conducted in polyethylene glycol demonstrated the presence of three Mg^{2+} binding sites [93], supporting the notion that Li^+ may compete in part for weakly bound Mg^{2+} in IMPase.

5.2.3 Inositol Depletion Hypothesis

Cellular concentrations of up to 10 mM Ins are found in the brain which reflect their importance in cell signaling [94]. One of the most appealing hypothesis for the mechanism of Li^+ action is the inositol depletion hypothesis. Ins represents the basis for two important signaling molecules, DAG and $InsP_3$. By inhibiting IMPase, Li^+ has been proposed to control the symptoms of bipolar disorder by depleting the cell of inositol, which in turn, would reduce the concentration of inositol-based secondary messengers such as DAG and PIP_2, preventing further signal transduction via PKC [96]. Several experiments with brain slices support this hypothesis [94].

The inositol depletion hypothesis does have some limitations. Klein and Melton demonstrated that Li^+ did not inhibit IMPase in *Xenopus* and proposed a new target for Li^+, glycogen synthase kinase-3(α) [97]. This has been further contradicted in genetic experiments which found that depletion of inositol had no effect on lithium-sensitive behavior [98].

5.3 Glycogen Synthase Kinase-3

GSK-3 is a constitutively active (no stimulation required) serine/threonine kinase. The name of the enzyme originates from a function that was early discovered: regulation of glycogen levels through inhibition of glycogen synthase. To regulate GSK-3 in this system, GSK is inhibited by insulin [99]. Extensive studies have provided evidence of GSK-3 functioning as an important regulatory kinase in a number of important roles, including inflammation, apoptosis, embryonic development, heart function, and synaptic transmission in neurons [100–105]. In fact, GSK-3 has now been shown to phosphorylate at least 50 different proteins, thus providing important regulation in an array of signaling pathways vital for homeostasis. Improper regulation on the part of GSK-3 can lead to a number of disease states. Indeed, hyperactive GSK-3 has been linked to several devastating illnesses including: Alzheimer's disease [101], diabetes [102], cancer [100, 106], Huntington's disease [107], and schizophrenia [108], to name a few.

GSK-3β can be found in the cytosol and in the nucleus as well as in mitochondria. It exists in two different splice variants GSK-3β1 and GSK-3β2. GSK-3β1 is a

shorter variant and lacks exon 9 (a 13-residue exon), whereas GSK-3β2 is longer and does contain the 13-residue exon 9 in the catalytic domain [109]. While GSK-3β1 is expressed ubiquitously, GSK-3β2 is expressed almost exclusively in the central nervous system during development as well as into adulthood [109, 110]. The function of exon 9 in GSK-3β2 is still poorly understood. Unless otherwise stated, the rest of this section will be referring to GSK-3β1.

5.3.1 Mechanism of Glycogen Synthase Kinase-3

Serine/threonine kinases typically utilize a combination of alpha helices and beta sheets, which must be aligned in a specific orientation for enzymatic activity. GSK-3β does contain moieties with these unique secondary structural motifs. Most kinases use phosphorylated residues in an allosteric activation domain to achieve an active conformation. GSK-3 is more tightly regulated and phosphorylation may inhibit or activate it depending on the phosphorylation site. GSK-3 is inactivated when phosphorylated at the amine terminal serine (S) 9 in GSK-3β or at S21 in GSK-3α (Figure 6). When phosphorylated at these residues, a primed pseudo-substrate is formed in the active site, which acts as a competitive inhibitor [111]. In contrast, phosphorylation at tyrosine (Y) 216 in GSK-3β or Y279 in GSK-3α seems to promote activity, but because GSK-3 is a constitutively active enzyme it is unknown how important this phosphorylation actually is for activity [112].

Crystal structure analysis shows another unique trait of GSK-3β in that it prefers a phosphoserine on the substrate. More specifically, GSK-3 recognizes the sequence S/TXXXS, in which the P + 4 serine has been previously phosphorylated by another kinase. When the substrate has been "primed" by a prior phosphorylation event, GSK-3β is found to be exponentially more efficient [112, 113].

5.3.2 Li^+ Inhibition of Glycogen Synthase Kinase-3β

Like any important enzyme, GSK-3β activity must be closely regulated. Cells have four mechanisms for regulating GSK-3: phosphorylation of GSK-3β itself, phosphorylation of the substrate, subcellular localization and the formation of protein complexes [114]. For the native enzyme, the most effective mechanism of regulation is through phosphorylation of key residues in GSK-3. Inhibition of GSK-3β has therefore become a research topic of much significance. Li^+ has been shown to inhibit GSK-3β and is effective in the 1–2 mM range [97]; therefore, GSK-3β is significantly inhibited by Li^+ at therapeutically relevant concentrations.

There has been much debate as to the exact composition of the active site but what is known is that the active site of GSK-3β requires a Mg^{2+} cofactor to function. Li^+ is a noncompetitive inhibitor of GSK-3β with respect to substrate [97] but evidence has shown that Li^+ is a competitive inhibitor with respect to Mg^{2+} [115, 116]. This is a fairly unusual mechanism in that Li^+ binds the enzyme-substrate complex by partially displacing Mg^{2+} from the active site [97]. Because Li^+ and Mg^{2+} are

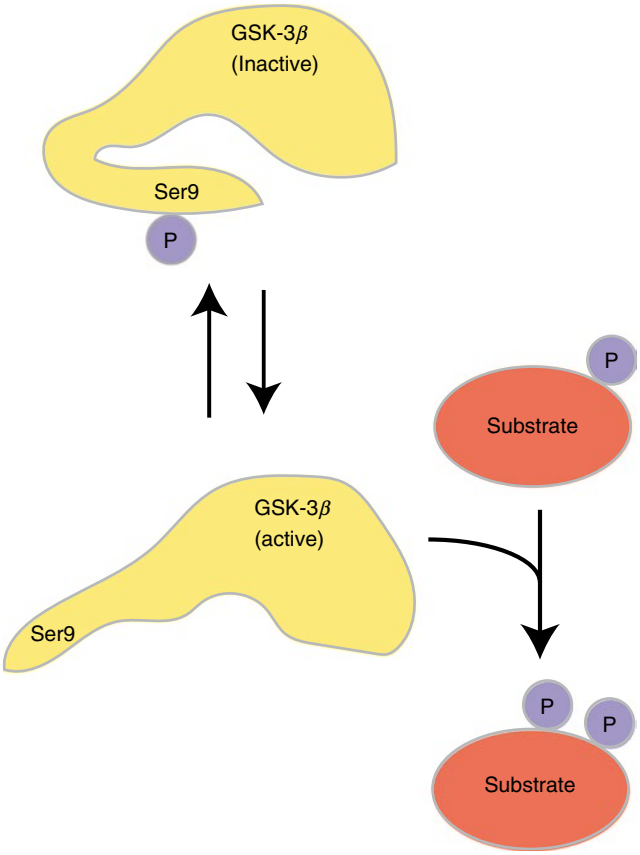

Figure 6 Roles of phosphorylation and dephosphorylation in the activity of GSK-3β. The N-terminus of GSK-3β acts as a pseudo-substrate and sterically hinders the active site when phosphorylated at Ser9. Upon dephosphorylation, the pseudo-substrate sways away from the active site making it accessible to the substrate. Active GSK-3β prefers to phosphorylate primed substrates.

similar in atomic radius, and both are positively charged, Li^+ is thought to be able to fit in the active site and displace, in part, the Mg^{2+} ion.

GSK-3 has been crystallized by several research groups. Figure 7 shows that, in the case of the ADP-bound structure the active site contains a mononuclear Mg^{2+} center in which a solvent-accessible cleft is lined with an aspartate and an asparagine residue [117]. In contrast, when an ATP analog is bound, an additional aspartate is present forming a binuclear Mg^{2+} center [118].

There has been much effort put into developing inhibitors of GSK-3 due to its involvement in a wide array of diseases. Design of such inhibitors has been met with challenges. Surrounding hydrophobic residues make accurately targeting the active site difficult [119].

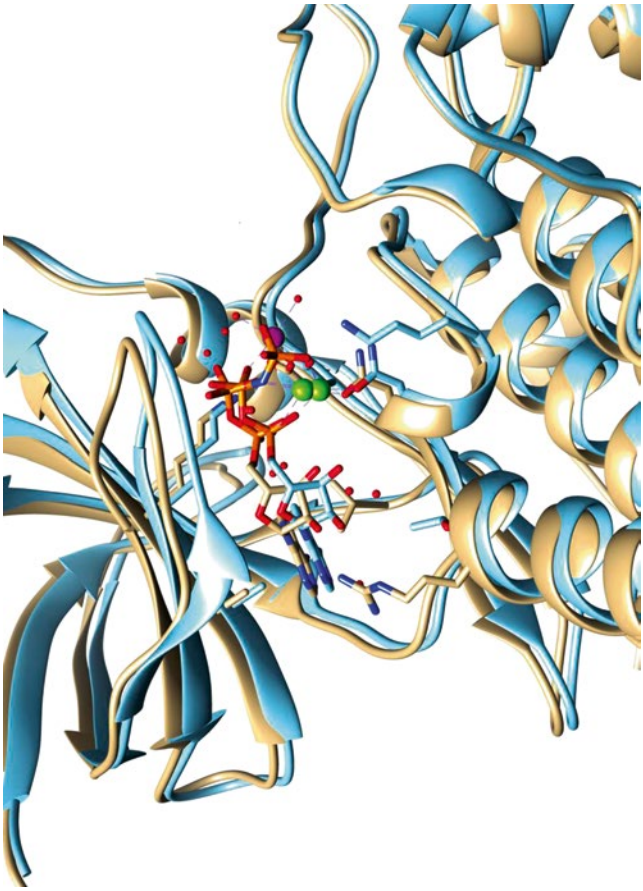

Figure 7 Crystallographic studies have shown GSK-3 to have mononuclear Mg^{2+} when ADP is bound in the active site (gold structure; Mg^{2+}, magenta). In contrast, when an ATP analog is bound, a dinuclear Mg^{2+} center (green) was observed (blue structure). Courtesy of the Protein Data Bank with the entries 1J1C (gold) [111], 1PYX (blue) [112]. Molecular graphics and analyses were performed with the UCSF Chimera package. Chimera is developed by the Resource for Biocomputing, Visualization, and Informatics at the University of California, San Francisco (supported by NIGMS P41-GM103311) [131].

5.4 Protein Kinase C and Myristoylated Alanine-Rich C-Kinase Substrate

The protein kinase C superfamily has been studied for many years and has greatly improved our knowledge of cell signaling and the use of secondary messengers within the cell. All isoforms of PKC contain a catalytic domain as well as a regulatory domain but their regulatory domains differ considerably in their primary structure. These differences dictate the activators that will bind to the mature enzyme.

PKC plays such a central role in cell signaling and is involved in many cellular functions. It is therefore not surprising that improper regulation of PKC has been observed in many diseases ranging from cancer [120] to BD [120, 121]. The first level of regulation is a maturation process that all PKC isoforms must undergo before they become active. Like GSK-3β, PKC also contains an autoinhibitory sequence (i.e., a pseudosubstrate) in the regulatory moiety that sterically hinders the active site, and must first be removed. This is accomplished by having a cofactor bind to the regulatory moiety [122]. At rest, PKC can be membrane-bound but is predominantly found in the cytosol [123]. PKC must also be phosphorylated at key residues and translocated to the membrane before it can be active [122, 124]. These post-translational modifications are necessary to correctly position key residues within the catalytic domain and to free the necessary space in the active site. PKC can be activated by certain upstream kinases including GPCRs, receptor tyrosine kinases, Ca^{2+}, and, depending on the isoform, DAG [120, 125]. Once activated, PKC can respond to secondary messengers and phosphorylate a number of specific downstream substrates, which, in turn, can regulate a variety of cell signaling pathways [122], one being the Wnt pathway of which is GSK-3β is a part [126, 127].

Myristoylated alanine-rich C-kinase substrate (MARCKS) is a highly conserved yet unstructured membrane-bound 32kD protein that is a common protein substrate for PKC and is myristoylated at the N-terminus. In addition to the N-terminal myristate, an acidic domain is crucial for MARCKS to bind negatively charged phospholipids in the membrane such as PIP_2. MARCKS and PKC colocalize on the membrane, allowing PKC to become active [128, 129]. Chronic Li^+ use has shown to inhibit PKC indirectly by altering the transcription levels of MARCKS, the key PKC substrate [130].

6 Concluding Remarks and Future Directions

With the exception of its general ability to compete with bound Mg^{2+} in Mg^{2+}-containing enzymes, Li^+ is a promiscuous inorganic ion that lacks binding specificity. However, recent theoretical studies have shed light on factors that may afford Li^+ affinity for cellular targets: (i) exposure of the Li^+ binding sites to solvent; (ii) the amino acids involved in metal ion coordination; and (iii) the net positive charge of a buried binding site [10]. Li^+ salts are, however, toxic drugs.

The understanding from Li^+ interactions with the cellular targets that have been identified may provide leads for the development of organic-based drugs with lower toxicity and higher specificity for GSK-3β and IMPase. Medication alone is not the only avenue that should be pursued when treating the chemical imbalance that is the hallmark of bipolar disorder. Patients with this illness must work closely with psychiatrists or psychologists in order to develop the tools for recognizing and seeking help for impending manic or depressive episodes [14].

Abbreviations

Aβ	amyloid β-peptides
AC	adenylyl cyclase
AD	Alzheimer's disease
ATP	adenosine 5′-triphosphate
[B]	concentration of binding sites
BD	bipolar disorder
BDNF	brain-delivered neurotropic factor
cAMP	3,5′-cyclic adenosine monophosphate
cP	centipoise, a unit of viscosity
CREB	cAMP response element-binding protein
DAG	1,2-diacylglycerol
$[Dy(PPP)_2]^{7-}$	dysprosium triphosphate
G_{α}	G-protein α subunit
$G_{\alpha s}$	G-protein αs subunit (AC stimulatory)
$G_{\alpha q}$	G-protein αq isoform (IMPase stimulatory)
$G_{i\alpha 1}$	G-protein iα1 isoform (AC inhibitor)
G-proteins	guanine nucleotide binding proteins
GDP	guanosine 5'-diphosphate
GPCR	G-protein coupled receptor
GSK-3	glycogen synthase kinase-3
GSK-3α	glycogen synthase kinase-3α
GSK-3β	glycogen synthase kinase-3β
GSK-3β1	glycogen synthase kinase-3β1
GSK-3β2	glycogen synthase kinase-3β2
GTP	guanosine 5' -triphosphate
HEPES	4-(2-hydroxyethyl)piperazine-1-ethanesulfonic acid
$HTm(DOTP)^{4-}$	thulium 1,4,7,10-tetraazacyclodecane-*N′,N″,N‴*-tetramethylene-phosphonate
IMPase	inositol monophosphatase
InsP	inositol phosphate
$InsP_2$	4,5-inositol bisphosphate
$InsP_3$	1,4,5-inositol triphosphate
K_{Li}	Li^+ binding constant
K_d	dissociation constant of the furaptra complex with Mg^{2+}
K_d'	dissociation constant of the furaptra complex with Li^+
K_i	inhibition constant
$[Li^+]_{bound}$	bound lithium concentration
$[Li^+]_{free}$	free lithium concentration
$[Li^+]_{total}$	total lithium concentration
MARCKS	myristoylated alanine-rich C-kinase
$[Mg^{2+}]_{bound}$	bound magnesium concentration
$[Mg^{2+}]_{free}$	free magnesium concentration

$[Mg^{2+}]_{total}$	total magnesium concentration
MHz	megahertz (10^9 s^{-1})
MRSI	magnetic resonance with spectroscopic imaging
Msec	millisecond (10^{-3} seconds)
NMR	nuclear magnetic resonance spectroscopy
PI	phosphatidylinositol
PIP_2	phosphatidylinositol 4,5-bisphosphate
PKA	protein kinase A
PKC	protein kinase C
PLC	phospholipase C
pm	picometer (10^{-12} meter)
r	ionic radius
R	fluorescence intensity ratios observed for the sample
RBC	red blood cell
R_{bound}	relaxation rate (reciprocal of T_1) for bound Li^+
R_{free}	relaxation rate (reciprocal of T_1) with saturating $[Li^+]_{total}$
R_{max}	fluorescence intensity ratio in the presence of saturating amounts of Mg^{2+}
R'_{max}	fluorescence intensity ratio in the presence of saturating concentrations of Li^+
R_{min}	fluorescence intensity ratios in the absence of Mg^{2+} and Li^+
R_{obs}	relaxation rate (reciprocal of T_1) observed with the NMR sample
Ser, S	serine
S_{min}	fluorescence intensity in the absence of Mg^{2+} and Li^+
S_{max}	fluorescence intensity in the presence of saturating concentrations of Mg^{2+}
S'_{max}	fluorescence intensity in the presence of saturating concentrations of Li^+
T_1	spin-lattice relaxation time
T_2	spin-spin relaxation time
T3	triiodothyrosine
T4	thyroxine
Tris	tris(hydroxymethyl)aminomethane
τ_c	correlation time
UV/Vis	ultra-violet/visible spectroscopy
ω	NMR resonance frequency
Tyr, Y	tyrosine

Acknowledgments Work in our laboratory is a culmination of a thirty-plus effort on the part of very capable graduate and undergraduate students, and postdoctoral fellows, and a long collaboration with Professor Margarida Castro and Professor Carlos Geraldes from the University of Coimbra, Portugal. Professor Mota de Freitas acknowledges that, without their talent and dedication, the projects described herein would not have come to fruition. We are grateful for funding from the Research Cooperation, the American Heart Association of Metropolitan Chicago, NATO (CRG921011), and the National Institute of Mental Health (MH45926).

References

1. Z. Rappoport, I. Marek, *The Chemistry of Organolithium Compounds,* John Wiley & Sons, 2004.
2. G. Eichinger, J. O. Besenhard, *J. Electroanal. Chem. Interfacial Electrochem.* **1976,** *72,* 1–31.
3. S. Huang, P. Cao, C. Wang, Z. Huang, W. Gao, *J. As. Cer. Soc.* **2013,** *1,* 46–52.
4. F. Barnaby, *How Nuclear Weapons Spread: Nuclear-Weapon Proliferation in the 1990s,* Routledge, London, 2012.
5. R. Shannon, *Acta Cryst.* **1976,** *A32,* 751–767.
6. J. Mahler, I. Persson, *Inorg. Chem.* **2012,** *51,* 425–438.
7. T. Dudev, J. A. Cowan, C. Lim, *J. Am. Chem. Soc.* **1999,** *121,* 7665–7673.
8. D. Mota de Freitas, M. M. Castro, C. F. Geraldes, *Acc. Chem. Res.* **2006,** *39,* 283–291.
9. J. J. Frausto da Silva, R. J. P. Williams, *Nature* **1976,** *263,* 237–239.
10. T. Dudev, C. Lim, *J. Am. Chem. Soc.* **2011,** *133,* 9506–9515.
11. G. S. Malhi, M. Tanious, D. Bargh, P. Das, M. Berk, *Aust Prescr.* **2013,** *36,* 18–21.
12. W. Jahnen-Dechent, M. Ketteler, *Clin. Kidney J.* **2012,** *5,* i3–i14.
13. H. Ohgami, T. Terao, I. Shiotsuki, N. Ishii, N. Iwata, *Br. J. Psychiatry* **2009,** *194,* 464–465; discussion 446.
14. American Psychiatric Association, *Diagnostic and Statistical Manual of Mental Disorders, (DSM-5),* American Psychiatric Pub., 2013.
15. E. Walker, R. E. McGee, B. G. Druss, *JAMA Psychiatry* **2015,** *72,* 334–341.
16. L. H. Price, G. R. Heninger, *N. Engl. J. Med.* **1994,** *331,* 591–598.
17. T. Suppes, R. J. Baldessarini, G. L. Faedda, M. Tohen, *Arch. Gen. Psychiatry* **1991,** *48,* 1082–1088.
18. K. N. Fountoulakis, E. Vieta, M. Siamouli, M. Valenti, S. Magiria, T. Oral, D. Fresno, P. Giannakopoulos, G. S. Kaprinis, *Ann. Gen. Psychiatry* **2007,** *6,* 27.
19. M. C. Wong, *Indian J. Psychol. Med.* **2011,** *33,* 18–28.
20. K. N. Fountoulakis, E. Vieta, *Imt. J. Neuropsychopharmacol.* **2008,** *11,* 999–1029.
21. L. V. Kessing, L. Sondergard, J. L. Forman, P. K. Andersen, *Arch. Gen. Psychiatry* **2008,** *65,* 1331–1335.
22. R. Nitrini, P. Caramelli, E. Herrera Jr, V. S. Bahia, L. F. Caixeta, M. Radanovic, R. Anghinah, H. Charchat-Fichman, C. S. Porto, M. T. Carthery, A. P. Hartmann, N. Huang, J. Smid, E. P. Lima, L. T. Takada, D. Y. Takahashi, *Alzheimer Dis. Assoc. Disord.* **2004,** *18,* 241–246.
23. M. Hong, D. C. Chen, P. S. Klein, V. M. Lee, *J. Biol. Chem.* **1997,** *272,* 25326–25332.
24. S. Lovestone, D. R. Davis, M. T. Webster, S. Kaech, J. P. Brion, A. Matus, B. H. Anderton, *Biol. Psychiatry* **1999,** *45,* 995–1003.
25. J. R. Munoz-Montano, F. J. Moreno, J. Avila, J. Diaz-Nido, *FEBS Lett.* **1997,** *411,* 183–188.
26. L. Trujillo-Estrada, S. Jimenez, V. De Castro, M. Torres, D. Baglietto-Vargas, I. Moreno-Gonzalez, V. Navarro, R. Sanchez-Varo, E. Sanchez-Mejias, J. C. Davila, M. Vizuete, A. Gutierrez, J. Vitorica, *Acta Neuropathol. Commun.* **2013,** *1,* 73.
27. C. Parr, R. Carzaniga, S. M. Gentleman, F. Van Leuven, J. Walter, M. Sastre, *Mol. Cell. Biol.* **2012,** *32,* 4410–4418.
28. C. Feyt, P. Kienlen-Campard, K. Leroy, F. N'Kuli, P. J. Courtoy, J. P. Brion, J. N. Octave, *J. Biol. Chem.* **2005,** *280,* 33220–33227.
29. A. Caccamo, S. Oddo, L. X. Tran, F. M. LaFerla, *Am. J. Pathol.* **2007,** *170,* 1669–1675.
30. M. A. Nunes, T. A. Viel, H. S. Buck, *Curr. Alzheimer Res.* **2013,** *10,* 104–107.
31. O. V. Forlenza, V. J. De-Paula, B. S. Diniz, *ACS Chem. Neurosci.* **2014,** *5*, 443–450.
32. J. Kohrle, *Mol. Cell. Endocrinol.* **1999,** *151,* 103–119.
33. S. C. Berens, R. S. Bernstein, J. Robbins, J. Wolff, *J. Clin. Invest.* **1970,** *49,* 1357–1367.
34. C. H. Emerson, A. J. Anderson, W. J. Howard, R. D. Utiger, *J. Clin. Endocrinol. Metab.* **1975,** *40,* 33–36.

35. D. Barbaro, G. Boni, G. Meucci, U. Simi, P. Lapi, P. Orsini, C. Pasquini, F. Piazza, M. Caciagli, G. Mariani, *J. Clin. Endocrinol. Metab.* **2003,** *88,* 4110–4115.
36. D. Mota de Freitas, M. Espanol, E. Dorus, *in Lithium Transport in Red Blood Cells of Bipolar Patients,* Vol. 4 of *Lithium and the Blood,* Eds F. Johnson, V. Gallicchio, Karger, Basel, 1991, pp. 96–120.
37. G. D. Christian, *J. Pharm. Biomed. Anal.* **1996,** *14,* 899–908.
38. C. J. Jameson, J. Mason, *in The Parameters of NMR Spectroscopy, Multinuclear NMR,* Ed J. Mason, Plenum Press, New York, 1987, pp. 3–50.
39. H. Günther, *in Advanced Applications of NMR to Organometallic Chemistry,* Eds B. Wrackmeyer, M. Gielen, R. Willem, Wiley, Chichester, UK, 1996, pp. 247–290.
40. V. Saudek, P. Vincendon, Q. T. Do, R. A. Atkinson, V. Sklenar, P. D. Pelton, F. Piriou, A. J. Ganzhorn, *Eur. J. Biochem.* **1996,** *240,* 288–291.
41. A. Haimovich, U. Eliav, A. Goldbourt, *J. Am. Chem. Soc.* **2012,** *134,* 5647–5651.
42. D. Mota de Freitas, *in Alkali Metal Nuclear Magnetic Resonance,* Vol. 227 of *Methods in Enzymology: Metallobiochemistry Part D: Physical and Spectroscopic Methods for Probing Metal Ion Environments in Metalloproteins,* Eds J. F. Riordan, B. L. Vallee, Academic Press, Waltham, USA, 1993, pp. 78–106.
43. M. C. Espanol, D. Mota de Freitas, *Inorg. Chem.* **1987,** *26,* 4356–4359.
44. Q. Rong, M. Espanol, D. Mota de Freitas, C. F. Geraldes, *Biochemistry* **1993,** *32,* 13490–13498.
45. T. L. James, J. H. Noggle, *Proc. Natl. Acad. Sci. USA* **1969,** *62,* 644–649.
46. J. Lee, C. Adler, M. Norris, W. Chu, E. M. Fugate, S. M. Strakowski, R. A. Komoroski, *Magn. Reson. Med.* **2012,** *68,* 363–368.
47. B. Raju, E. Murphy, L. A. Levy, R. D. Hall, R. E. London, *Am. J. Physiol.* **1989,** *256,* C540–C548.
48. D. Mota de Freitas, L. Amari, C. Srinivasan, Q. Rong, R. Ramasamy, A. Abraha, C. F. Geraldes, M. K. Boyd, *Biochemistry* **1994,** *33,* 4101–4110.
49. C. S. Malarkey, G. Wang, M. A. Ballicora, D. Mota de Freitas, *Biochem. Biophys. Res. Commun.* **2008,** *372,* 866–869.
50. J. Nikolakopoulos, C. Zachariah, D. Mota de Freitas, E. B. Stubbs Jr, R. Ramasamy, M. C. Castro, C. F. Geraldes, *J. Neurochem.* **1998,** *71,* 1676–1684.
51. Y. Chi, S. Mo, D. Mota de Freitas, *Biochemistry.* **1996,** *35,* 12433–12442.
52. M. Canessa, N. Adragna, H. S. Solomon, T. M. Connolly, D. C. Tosteson, *N. Engl. J. Med.* **1980,** *302,* 772–776.
53. B. T. Layden, N. Minadeo, J. Suhy, A. M. Abukhdeir, T. Metreger, K. Foley, G. Borge, J. W. Crayton, F. B. Bryant, D. M. d. Freitas, *Bipolar Disord.* **2004,** *6,* 53–61.
54. L. P. Montezinho, C. B Duarte, C. P. Fonseca, Y. Glinka, B. Layden, D. Mota de Freitas, C. F. Geraldes, M. M. Castro, *J. Neurochem.* **2004,** *90,* 920–930.
55. B. T. Layden, A. M. Abukhdeir, C. Malarkey, L. A. Oriti, W. Salah, C. Stigler, C. F. Geraldes, D. Mota de Freitas, *Biochim. Biophys. Acta* **2005,** *1741,* 339–349.
56. A. M. Abukhdeir, B. T. Layden, N. Minadeo, F. B. Bryant, E. B. Stubbs, D. Mota de Freitas, *Bipolar Disord.* **2003,** *5,* 6–13.
57. J. C. Soares, F. Boada, M. S. Keshavan, *Eur. Neuropsychopharmacol.* **2000,** *10,* 151–158.
58. J. Baek, G. Kinrys, A. Nierenberg, *Acta Psychiatr. Scand.* **2014,** *129,* 17–23.
59. L. Carter, M. Zolezzi, A. Lewczyk, *Can. J. Psychiatry* **2013,** *58,* 595–600.
60. E. D. Peselow, D. L. Dunner, R. R. Fieve, A. Lautin, *J. Affect. Disord.* **1980,** *2,* 303–310.
61. M. Jafferany, *Int. J. Dermatol.* **2008,** *47,* 1101–1111.
62. A. Nassar, A. N. Azab, *ACS Chem. Neurosci.* **2014**, *5*, 451–458.
63. P. R. Leeds, F. Yu, Z. Wang, C. T. Chiu, Y. Zhang, Y. Leng, G. R. Linares, D. M. Chuang, *ACS Chem. Neurosci.* **2014,** *5,* 422–433.
64. T. M. Cabrera-Vera, J. Vanhauwe, T. O. Thomas, M. Medkova, A. Preininger, M. R. Mazzoni, H. E. Hamm, *Endocr. Rev.* **2003,** *24,* 765–781.
65. J. Gonzalez-Maeso, J. J. Meana, *Curr. Neuropharmacol.* **2006,** *4,* 127–138.

66. S. Avissar, G. Schreiber, *Biol. Psychiatry* **1992,** *31,* 435–459.
67. S. Avissar, G. Schreiber, A. Danon, R. H. Belmaker, *Nature* **1988,** *331,* 440–442.
68. J. Gonzalez-Maeso, R. Rodriguez-Puertas, J. J. Meana, J. A. Garcia-Sevilla, J. Guimon, *Mol. Psychiatry.* **2002,** *7,* 755–767.
69. J. Ellis, R. H. Lenox, *Lithium* **1991,** *2,* 141–147.
70. H. Y. Wang, E. Friedman, *Neuropharmacology* **1999,** *38,* 403–414.
71. M. A. Pacheco, C. Stockmeier, H. Y. Meltzer, J. C. Overholser, G. E. Dilley, R. S. Jope, *Brain Res.* **1996,** *723,* 37–45.
72. E. Friedman, H. Y. Wang, *J. Neurochem.* **1996,** *67,* 1145–1152.
73. D. Dowlatshahi, G. M. MacQueen, J. F. Wang, J. S. Reiach, L. T. Young, *J. Neurochem.* **1999,** *73,* 1121–1126.
74. M. L. Wong, J. Licinio, *Nat. Rev. Drug Discov.* **2004,** *3,* 136–151.
75. H. K. Manji, R. H. Lenox, *Biol. Psychiatry* **2000,** *48,* 518–530.
76. H. K. Manji, J. A. Quiroz, J. L. Payne, J. Singh, B. P. Lopes, J. S. Viegas, C. A. Zarate, *World Psychiatry* **2003,** *2,* 136–146.
77. R. K. Sunahara, J. J. Tesmer, A. G. Gilman, S. R. Sprang, *Science.* **1997,** *278,* 1943–1947.
78. J. J. Tesmer, R. K. Sunahara, A. G. Gilman, S. R. Sprang, *Science.* **1997,** *278,* 1907–1916.
79. D. E. Coleman, A. M. Berghuis, E. Lee, M. E. Linder, A. G. Gilman, S. R. Sprang, *Science* **1994,** *265,* 1405–1412.
80. D. E. Coleman, S. R. Sprang, *Biochemistry* **1998,** *37,* 14376–14385.
81. D. E. Coleman, S. R. Sprang, *Meth. Enzymol.* **1999,** *308,* 70–92.
82. D. E. Coleman, E. Lee, M. B. Mixon, M. E. Linder, A. M. Berghuis, A. G. Gilman, S. R. Sprang, *J. Mol. Biol.* **1994,** *238,* 630–634.
83. N. I. Nicely, J. Kosak, V. de Serrano, C. Mattos, *Structure* **2004,** *12,* 2025–2036.
84. L. Mann, E. Heldman, Y. Bersudsky, S. F. Vatner, Y. Ishikawa, O. Almog, R. H. Belmaker, G. Agam, *Bipolar Disord.* **2009,** *11,* 885–896.
85. R. H. Belmaker, M. Kon, R. P. Ebstein, H. Dasberg, *Biol. Psychiatry* **1980,** *15,* 3–8.
86. J. Forn, F. G. Valdecasas, *Biochem. Pharmacol.* **1971,** *20,* 2773–2779.
87. R. P. Ebstein, A. Reches, R. H. Belmaker, *J. Pharm. Pharmacol.* **1978,** *30,* 122–123.
88. A. Reches, R. P. Ebstein, R. H. Belmaker, *Psychopharmacology (Berl).* **1978,** *58,* 213–216.
89. L. Mann, E. Heldman, G. Shaltiel, R. H. Belmaker, G. Agam, *Int. J. Neuropsychopharmacol.* **2008,** *11,* 533–539.
90. R. Machado-Vieira, H. K. Manji, C. A. Zarate, *Bipolar Disord.* **2009,** *11, Suppl 2,* 92–109.
91. M. J. Berridge, C. P. Downes, M. R. Hanley, *Cell* **1989,** *59,* 411–419.
92. J. R. Atack, H. B. Broughton, S. J. Pollack, *FEBS Lett.* **1995,** *361,* 1–7.
93. R. Gill, F. Mohammed, R. Badyal, L. Coates, P. Erskine, D. Thompson, J. Cooper, M. Gore, S. Wood, *Acta Crystallogr. D Biol. Crystallogr.* **2005,** *61,* 545–555.
94. A. J. Harwood, *Mol. Psychiatry* **2005,** *10,* 117–126.
95. R. Bone, J. P. Springer, J. R. Atack, *Proc. Natl. Acad. Sci. USA* **1992,** *89,* 10031–10035.
96. C. J. Phiel, P. S. Klein, *Annu. Rev. Pharmacol. Toxicol.* **2001,** *41,* 789–813.
97. P. S. Klein, D. A. Melton, *Proc. Natl. Acad. Sci. USA* **1996,** *93,* 8455–8459.
98. A. Shaldubina, R. A. Johanson, W. T. O'Brien, R. Buccafusca, G. Agam, R. H. Belmaker, P. S. Klein, Y. Bersudsky, G. T. Berry, *Mol. Genet. Metab.* **2006,** *88,* 384–388.
99. N. Embi, D. B. Rylatt, P. Cohen, *Eur. J. Biochem.* **1980,** *107,* 519–527.
100. J. A. McCubrey, L. S. Steelman, F. E. Bertrand, N. M. Davis, M. Sokolosky, S. L. Abrams, G. Montalto, A. B. D'Assoro, M. Libra, F. Nicoletti, R. Maestro, J. Basecke, D. Rakus, A. Gizak, Z. N. Demidenko, L. Cocco, A. M. Martelli, M. Cervello, *Oncotarget* **2014,** *5,* 2881–2911.
101. L. Martin, X. Latypova, C. M. Wilson, A. Magnaudeix, M. L. Perrin, C. Yardin, F. Terro, *Ageing Res. Rev.* **2013,** *12,* 289–309.
102. S. Amar, R. H. Belmaker, G. Agam, *Curr. Pharm. Des.* **2011,** *17,* 2264–2277.
103. C. Gao, C. Holscher, Y. Liu, L. Li, *Rev. Neurosci.* **2011,** *23,* 1–11.
104. H. Lal, F. Ahmad, J. Woodgett, T. Force, *Circ. Res.* **2015,** *116,* 138–149.

105. M. Llorens-Martin, J. Jurado, F. Hernandez, J. Avila, *Front. Mol. Neurosci.* **2014,** *7,* 46.
106. U. Maurer, F. Preiss, P. Brauns-Schubert, L. Schlicher, C. Charvet, *J. Cell. Sci.* **2014,** *127,* 1369–1378.
107. D. A. Perez-Martinez, *Neurologia* **2009,** *24,* 143–146.
108. A. R. Cole, *FEBS J.* **2013,** *280,* 5213–5227.
109. A. Wood-Kaczmar, M. Kraus, K. Ishiguro, K. L. Philpott, P. R. Gordon-Weeks, *Mol. Cell. Neurosci.* **2009,** *42,* 184–194.
110. F. Mukai, K. Ishiguro, Y. Sano, S. C. Fujita, *J. Neurochem.* **2002,** *81,* 1073–1083.
111. P. Cohen, S. Frame, *Nat. Rev. Mol. Cell Biol.* **2001,** *2,* 769–776.
112. R. Dajani, E. Fraser, S. M. Roe, N. Young, V. Good, T. C. Dale, L. H. Pearl, *Cell* **2001,** *105,* 721–732.
113. E. ter Haar, J. T. Coll, D. A. Austen, H. M. Hsiao, L. Swenson, J. Jain, *Nat. Struct. Biol.* **2001,** *8,* 593–596.
114. R. S. Jope, C. J. Yuskaitis, E. Beurel, *Neurochem. Res.* **2007,** *32,* 577–595.
115. W. J. Ryves, A. J. Harwood, *Biochem. Biophys. Res. Commun.* **2001,** *280,* 720–725.
116. W. J. Ryves, R. Dajani, L. Pearl, A. J. Harwood, *Biochem. Biophys. Res. Commun.* **2002,** *290,* 967–972.
117. M. Aoki, T. Yokota, I. Sugiura, C. Sasaki, T. Hasegawa, C. Okumura, K. Ishiguro, T. Kohno, S. Sugio, T. Matsuzaki, *Acta Crystallogr. D Biol. Crystallogr.* **2004,** *60,* 439–446.
118. J. A. Bertrand, S. Thieffine, A. Vulpetti, C. Cristiani, B. Valsasina, S. Knapp, H. M. Kalisz, M. Flocco, *J. Mol. Biol.* **2003,** *333,* 393–407.
119. H. C. Zhang, L. V. Bonaga, H. Ye, C. K. Derian, B. P. Damiano, B. E. Maryanoff, *Bioorg. Med. Chem. Lett.* **2007,** *17,* 2863–2868.
120. C. A. Zarate, H. K. Manji, *CNS Drugs* **2009,** *23,* 569–582.
121. R. S. Jope, *Mol. Psychiatry* **1999,** *4,* 117–128.
122. A. C. Newton, *J. Biol. Chem.* **1995,** *270,* 28495–28498.
123. H. K. Manji, R. H. Lenox, *Synapse* **1994,** *16,* 11–28.
124. A. C. Newton, J. E. Johnson, *Biochim. Biophys. Acta.* **1998,** *1376,* 155–172.
125. M. Serova, A. Ghoul, K. A. Benhadji, E. Cvitkovic, S. Faivre, F. Calvo, F. Lokiec, E. Raymond, *Semin. Oncol.* **2006,** *33,* 466–478.
126. N. Goode, K. Hughes, J. R. Woodgett, P. J. Parker, *J. Biol. Chem.* **1992,** *267,* 16878–16882.
127. H. K. Manji, R. H. Lenox, *Biol. Psychiatry* **1999,** *46,* 1328–1351.
128. J. M. Graff, J. I. Gordon, P. J. Blackshear, *Science* **1989,** *246,* 503–506.
129. A. Rosen, K. F. Keenan, M. Thelen, A. C. Nairn, A. Aderem, *J. Exp. Med.* **1990,** *172,* 1211–1215.
130. L. Wang, X. Liu, R. H. Lenox, *J. Neurochem.* **2001,** *79,* 816–825.
131. E. F. Pettersen, T. D. Goddard, C. C. Huang, G. S. Couch, D. M. Greenblatt, E. C. Meng, T. E. Ferrin, *J. Comput. Chem.* **2004,** *25,* 1605–1612.